the out-of-plane displacement **4a** as depicted in **7a**. The d_{yz}^-

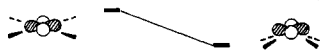

7a

7b

band at Γ has the nodal property shown in **8** along the *z* axis,

8

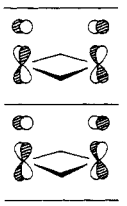

in which the interaction between Nb and O is antibonding within a chain but bonding between neighboring chains. Thus the out-of-plane Nb displacement **4a** would enhance the antibonding but decrease the bonding interaction. Figure 2 shows how the $d_{x^2-y^2}^+$ band top and the d_{yz}^- band bottom vary as a function of δ_2 when $\delta_1 = 0.2$ Å. As expected from the above discussion, the out-of-plane Nb displacement **4a** is found to slightly lower the $d_{x^2-y^2}^+$ band but greatly raise the d_{yz}^- band, eventually giving rise to a band gap beyond a certain value of δ_2. The repeat unit of the $NbOX_2$ net with $\delta_1 = 0$ and $\delta_2 \neq 0$ is $(NbOX_2)$, and thus there exists one electron per unit cell to fill the d-block bands. Such an $NbOX_2$ net cannot become semiconducting as in the case of NbX_4 chain with no Nb–Nb···Nb alternation.[6] Therefore, the out-of-plane Nb displacement is as crucial as the pairing distortion of Nb atoms for the semiconducting property of $NbOX_2$ net.

An alternative way of introducing Nb–O···Nb alternation into **3** is shown in **4b**, which shows a displacement of the oxygen atoms in each $NbOX_2$ chain of **3** toward the Nb atoms that are held in the X_4 planes. It is not **4b** but **4a** that is observed. The preference of **4a** over **4b** may be due in part to the stabilization of the $d_{x^2-y^2}^+$ band, which arises from the distortion **4a** as indicated in **7a**. When the Nb–O···Nb alternation is introduced as in **4b** into the $NbOX_2$ net with $\delta_1 = 0.2$ Å, our calculations show the $d_{x^2-y^2}^+$ and d_{yz}^- bands to remain overlapping for the oxygen atom displacement of as large as 0.2 Å. Incidently, the distortion **4a** leads to a rehybridization of the d_{yz} orbital as shown in **7b**. As a consequence of the energy level changes indicated in **7a** and **7b**, the distortion **4a** becomes more efficient than the alternative **4b** in introducing a band gap into $NbOX_2$ net.

Acknowledgment. This work was supported by the donors of the Petroleum Research Fund, administered by the American Chemical Society. The author wishes to thank Professor T. M. Rice for his valuable comment on this work. M.-H.W. is a Camille and Henry Dreyfus Teacher-Scholar, 1980–1985.

Registry No. $NbOCl_2$, 13867-44-2.

Contribution from the Francis Bitter National Magnet Laboratory, Massachusetts Institute of Technology, Cambridge, Massachusetts 02139, the Department of Chemistry, Harvard University, Cambridge, Massachusetts 02138, and Bell Laboratories, Murray Hill, New Jersey 07974

Antiferromagnetic Exchange Interactions in $[Fe_4S_4(SR)_4]^{2-,3-}$ Clusters

G. C. PAPAEFTHYMIOU,*[1a] E. J. LASKOWSKI,[1b] S. FROTA-PESSÔA,[1a] R. B. FRANKEL,[1a] and R. H. HOLM[1c]

Received July 27, 1981

The exchange coupling of Fe atoms in the mixed-valence clusters $[Fe_4S_4(SPh)_4]^{2-}$ and $[Fe_4S_4(SPh)_4]^{3-}$, synthetic analogues of [4Fe–4S] sites in ferredoxin proteins, has been examined in terms of a theoretical treatment of previously reported magnetic susceptibility and magnetization properties. Both clusters exhibit antiferromagnetic behavior at 4.2–338 K. The isotropic exchange Hamiltonian

$$\mathcal{H} = g\mu_B \sum_{i=1}^{4} \vec{H}\cdot\vec{S}_i - 2\sum_{i<j} J_{ij}\vec{S}_i\cdot\vec{S}_j$$

is used to parameterize the results in terms of the exchange constants J_{ij}. It is shown that a single value of J_{ij} does not produce satisfactory results for either cluster oxidation level. Allowing J_{ij} to have different values for coupled Fe sites in different combinations of Fe(II,III) oxidation states affords an accurate simulation of the temperature dependence of the magnetic susceptibility of $(Et_4N)_2[Fe_4S_4(SPh)_4]$. The best simulation was obtained with $J_{ij}(Fe^{3+} \rightleftarrows Fe^{3+}) = -275$ cm^{-1}, $J_{ij}(Fe^{2+} \rightleftarrows Fe^{2+}) = -225$ cm^{-1}, and $J_{ij}(Fe^{3+} \rightleftarrows Fe^{2+}) = -250$ cm^{-1}. For $(Et_4N)_3[Fe_4S_4(SPh)_4]$ a reasonable simulation of both the susceptibility and the magnetization results (at 4.2 K) was obtained with two independent J_{ij} values, $J_{ij}(Fe^{3+} \rightleftarrows Fe^{2+}) \approx -60$ cm^{-1} and $J_{ij}(Fe^{2+} \rightleftarrows Fe^{2+}) \approx -40$ cm^{-1}. The addition of a single electron to the [4Fe–4S] core unit is seen to produce a large decrease in the magnitude of the exchange constants. A similar behavior has been observed in the susceptibility properties of oxidized and reduced 2-Fe protein sites $[Fe_2S_2(Cys\text{-}S)_4]$. Limitations of the theoretical treatment are discussed.

Introduction

The synthesis and detailed structural and physicochemical characterization of the cubane-type clusters $[Fe_4S_4(SR)_4]^{2-,3-}$ have been previously reported.[2-11] These results have demonstrated the isoelectronic nature of the synthetic species with certain oxidation levels of the $[Fe_4S_4(Cys\text{-}S)_4]$ electron-transfer

(1) (a) Massachusetts Institute of Technology. (b) Bell Laboratories. (c) Harvard University.

(2) J. Cambray, R. W. Lane, A. G. Wedd, R. W. Johnson, and R. H. Holm, *Inorg. Chem.*, **16**, 2565 (1977).

(3) R. W. Lane, A. G. Wedd, W. O. Gillum, E. J. Laskowski, R. H. Holm, R. B. Frankel, and G. C. Papaefthymiou, *J. Am. Chem. Soc.*, **99**, 2350 (1977).

0020-1669/82/1321-1723$01.25/0

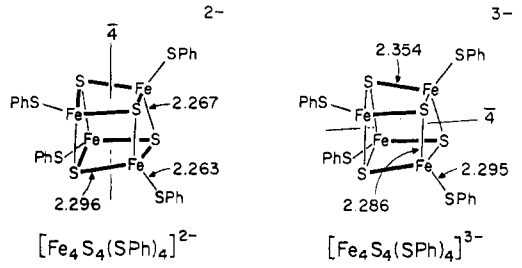

Figure 1. Schematic structures of $[Fe_4S_4(SPh)_4]^{2-,3-}$ clusters in the crystalline state presented in orientations of maximum congruence of the $[4Fe-4S]^{2+,1+}$ core units. Idealized symmetry axes and mean values of Fe–S distances are shown; dark lines depict the longer core Fe–S bond lengths.

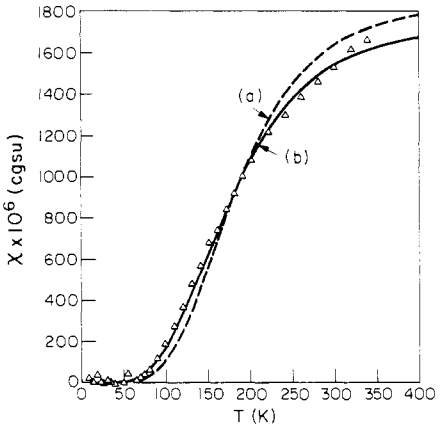

Figure 2. Temperature dependence of magnetic susceptibility per cluster for $(Et_4N)_2[Fe_4S_4(SPh)_4]$. Experimental points (Δ) have been corrected for an estimated apparent TIP of 440 × 10^{-6} cgsu: (a) best theoretical simulation for a single J value (−232 cm^{-1}); (b) best theoretical simulation with three values of exchange constants, J_1 = −275 cm^{-1}, J_2 = −225 cm^{-1}, J_3 = −250 cm^{-1}.

sites in ferredoxin (Fd) proteins. These oxidation levels are specified in eq 1 in terms of [4Fe–4S] core units, below which

$$\begin{aligned} Fd_{red}\ ([4Fe\text{–}4S]^{1+}) &\rightleftharpoons Fd_{ox}\ ([4Fe\text{–}4S]^{2+}) \\ [Fe_4S_4(SR)_4]^{3-} &\rightleftharpoons [Fe_4S_4(SR)_4]^{2-} \\ Fe(III) + 3Fe(II) & \quad 2Fe(III) + 2Fe(II) \end{aligned} \qquad (1)$$

are placed isoelectronic synthetic analogues of the sites and formal Fe oxidation states. In the crystalline state all dianion clusters exhibit an idealized tetragonal core structure compressed along the $\bar{4}$ symmetry axis, as illustrated for $[Fe_4S_4(SPh)_4]^{2-}$[9] in Figure 1. The reduced cluster $[Fe_4S_4(SPh)_4]^{3-}$, as its crystalline Et_3MeN^+ salt, also possesses a tetragonal core structure, which, however, is elongated along the $\bar{4}$ axis.[5] The clusters differ only slightly in structure, as seen from the ~0.06-Å difference in bonds approximately parallel to the $\bar{4}$ axis and a core volume increase of 0.18 Å^3 (1.9%) in passing from the oxidized to the reduced form. External constraints can modify core structures of various $[Fe_4S_4(SR)_4]^{3-}$ clusters,[5,7] but the elongated tetragonal geometry (or close approaches thereto) is uniformly adopted in solution.[5,7] Consequently, the structures in Figure 1 are considered the intrinsically stable forms of both analogue and protein site $[4Fe-4S]^{2+,1+}$ core units.

Both cluster oxidation levels are of the mixed-valence type but, on the basis of a variety of spectrocopic properties, are extensively delocalized. The clusters $[Fe_4S_4(SR)_4]^{2-}$ contain essentially equivalent Fe sites[9-11] with a mean Fe oxidation

Table I. Magnetic Data for $[Fe_4S_4(SPh)_4]^{2-,3-}$ Clusters[a] at Selected Temperatures

$[Fe_4S_4(SPh)_4]^{2-}$			$[Fe_4S_4(SPh)_4]^{3-}$		
T, K	$10^5\chi$,[b] cgsu	μ_{eff},[c] μ_B	T, K	$10^3\chi$,[b] cgsu	μ_{eff},[c] μ_B
50.2	44.0	0.42	4.2	125	2.05
75.2	48.5	0.54	10.5	57.4	2.19
100.2	63.1	0.71	29.4	25.8	2.46
120.3	80.8	0.88	50.2	17.4	2.64
140.3	101	1.06	75.2	13.5	2.85
160.4	118	1.23	100.2	11.5	3.03
180.4	136	1.40	130.3	10.3	3.27
200.4	152	1.56	150.4	9.78	3.43
240.3	174	1.83	180.4	9.02	3.62
279.5	190	2.06	200.4	8.70	3.73
299.1	196	2.17	240.3	8.28	3.99
338.1	210	2.38	279.5	7.94	4.21
			299.1	7.89	4.35
			338.1	7.63	4.54

[a] Data presented for both anions are for their Et_4N^+ salts.[5] [b] Susceptibility is given per 4 Fe atoms of the tetrameric unit. [c] $\mu_{eff} = 2.828(\chi T)^{1/2}$.

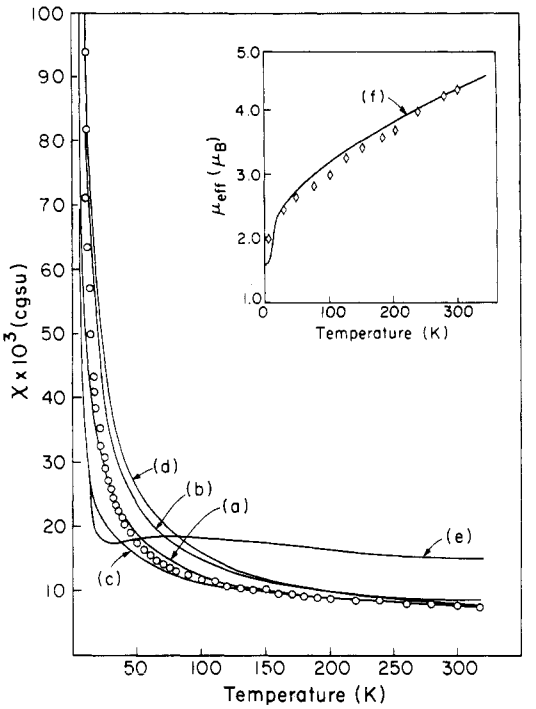

Figure 3. Temperature dependence of magnetic susceptibility ((○) experimental points) and effective magnetic moment (inset: (◇) experimental points) per cluster for $(Et_4N)_3[Fe_4S_4(SPh)_4]$. The solid lines are theoretical simulations with one or two values of J, as follows: (a) J_1 = −60 cm^{-1}, J_2 = −40 cm^{-1}, best fit; (b) J_1 = −60 cm^{-1}, J_2 = −38 cm^{-1}; (c) J_1 = −60 cm^{-1}, J_2 = −42 cm^{-1}; (d) J_1 = −65 cm^{-1}, J_2 = −40 cm^{-1}; (e) J = −20 cm^{-1} (single value of J); (f) (inset) J_1 = −60 cm^{-1}, J_2 = −40 cm^{-1}.

(4) J. G. Reynolds, E. J. Laskowski, and R. H. Holm, *J. Am. Chem. Soc.*, **100**, 5315 (1978).
(5) E. J. Laskowski, R. B. Frankel, W. O. Gillum, G. C. Papaefthymiou, J. Renaud, J. A. Ibers, and R. H. Holm, *J. Am. Chem. Soc.*, **100**, 5322 (1978).
(6) J. M. Berg, K. O. Hodgson, and R. H. Holm, *J. Am. Chem. Soc.*, **101**, 4586 (1979).
(7) E. J. Laskowski, J. G. Reynolds, R. B. Frankel, S. Foner, G. C. Papaefthymiou, and R. H. Holm, *J. Am. Chem. Soc.*, **101**, 6562 (1979).
(8) G. C. Papaefthymiou, R. B. Frankel, S. Foner, E. J. Laskowski, and R. H. Holm, *J. Phys. Colloq. (Orsay, Fr.)*, **41**, C1-493 (1980).
(9) L. Que, Jr., M. A. Bobrik, J. A. Ibers, and R. H. Holm, *J. Am. Chem. Soc.*, **96**, 4168 (1974).
(10) R. B. Frankel, B. A. Averill, and R. H. Holm, *J. Phys. (Orsay, Fr.)*, **35**, C6-107 (1974).
(11) R. H. Holm, B. A. Averill, T. Herkovitz, R. B. Frankel, H. B. Gray, O. Siiman, and F. T. Grunthaner, *J. Am. Chem. Soc.*, **96**, 2644 (1974).

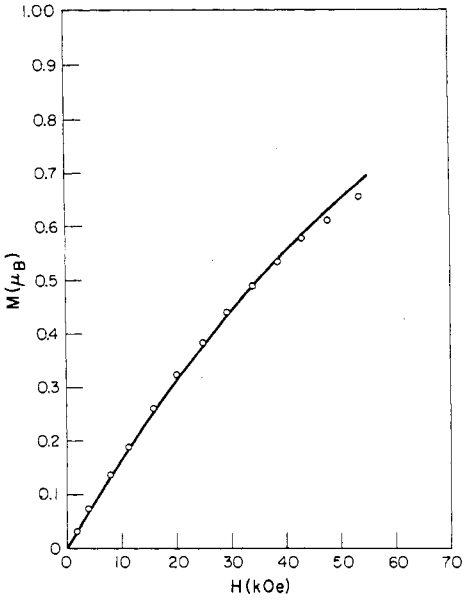

Figure 4. Magnetization vs. applied field at T = 4.2 K for $(Et_4N)_3[Fe_4S_4(SPh)_4]$: (O) experimental data; (—) theoretical simulation with $J_1 = -60$ cm^{-1}, $J_2 = -40$ cm^{-1}.

state of +2.5. Negative spin-exchange interactions result in a singlet ground state and an array of integral spin excited states. The absence of an EPR signal and magnetic hyperfine interaction in Mössbauer spectra reveal that only the ground state is appreciably populated at 4.2 K. Magnetic susceptibility (χ) results for $[Fe_4S_4(SPh)_4]^{2-}$ at 50–338 K,[5] shown in Figure 2 and Table I, indicate increasing effective moment per cluster (μ_{eff}) with increasing temperature, corresponding to the population of higher spin states. The reduced clusters $[Fe_4S_4(SR)_4]^{3-}$, having a mean Fe oxidation state of +2.25, exhibit different physical properties in the solid state dependent upon tetragonal vs. nontetragonal core structures.[5,7] Mössbauer spectra of salts of $[Fe_4S_4(SPh)_4]^{3-}$ at low temperature reveal two magnetically inequivalent Fe sites with hyperfine interactions of different magnitude and opposite sign, corresponding to antiparallel spin coupling. This interaction produces a doublet ground state ($g_\parallel = 2.05$, $g_\perp = 1.93$ in frozen solution[5]) and a spectrum of excited half-integral spin states. The $\chi(T)$ behavior of $[Fe_4S_4(SPh)_4]^{3-}$, shown in Figure 3 and Table I, is consistent with the occupation of higher spin states as the temperature is increased. Magnetization results at fields up to 50 kOe at 4.2 K, given in Figure 4, suggest a moment per cluster approaching 1 μ_B, corresponding to a $S = {}^1/_2$ ground state.

Earlier we had reported detailed $\chi(T)$ data for a number of $[Fe_4S_4(SR)_4]^{2-,3-}$ salts, all of which displayed antiferromagnetic behavior, and demonstrated that both susceptibility and magnetization properties differed between tetragonal and nontetragonal cluster trianions.[5,7] Other than the observation that the conventional antiferromagnetic coupling model[12] with a single exchange constant J does not reproduce the susceptibility results satisfactorily,[5,8] no attempts were made to analyze the $\chi(T)$ data in greater detail. Here we report the parameterization of the magnetic susceptibility data for $[Fe_4S_4(SPh)_4]^{2-,3-}$ and the magnetization data for the trianion cluster by analysis with a Heisenberg exchange Hamiltonian, characterized by exchange coupling constants J_{ij}. The analysis indicates that the addition of an electron passing from dianion to trianion results in an approximately fivefold decrease in the magnitudes of the exchange parameters J_{ij}.

(12) W. E. Hatfield, in "Theory and Applications of Molecular Paramagnetism", E. A. Boudreaux and L. N. Mulay, Eds., Wiley-Interscience, New York, 1976, Chapter 7.

Theoretical Considerations

The simple isotropic exchange Hamiltonian expressed by eq 2 is used to parameterize the exchange among Fe atoms

$$\mathcal{H} = g\mu_B\sum_{i=1}^{4}\vec{H}\cdot\vec{S}_i - 2\sum_{i<j}J_{ij}\vec{S}_i\cdot\vec{S}_j \qquad (2)$$

in a cluster and to simulate the $\chi(T)$ data of the clusters in the two oxidation levels. The first term gives the Zeeman interaction of the Fe spins with the applied magnetic field H, assumed in the z direction, and allows the calculation of the magnetization of the 4-Fe system at different values of applied field. The second term is the isotropic exchange interaction. In eq 2 g is the electronic gyromagnetic ratio, μ_B is the Bohr magneton, $\vec{S}_i$ is the spin on the ith Fe atom, and J_{ij} is the exchange integral coupling atoms i and j with total spins $\vec{S}_i$, $\vec{S}_j$. The sign of J_{ij} is positive for parallel and negative for antiparallel spin coupling.

While Mössbauer spectral and other experimental evidence indicates a high degree of electron delocalization in both cluster oxidation levels, we assume Fe(II) and Fe(III) sites with localized spins of $S = 2$ and $S = {}^5/_2$, respectively, in simulating the $\chi(T)$ data. Furthermore, interactions between clusters are assumed to be negligible compared to the interactions among Fe atoms within a cluster. $\mathcal{H}$ operates on the spin wave functions in the uncoupled basis set obtained as product states of individual Fe spin states $|S_i,S_{iz}\rangle$. Thus, $S_1 = S_2 = {}^5/_2$ and $S_3 = S_4 = 2$ for the cluster dianion and $S_1 = {}^5/_2$ and $S_2 = S_3 = S_4 = 2$ for the cluster trianion. This results in a 900 × 900 spin matrix for the former and a 750 × 750 spin matrix for the latter cluster. The eigenvalue problem is greatly simplified by the fact that if only isotropic Zeeman and exchange interactions are considered, these matrices can be block-factored, thereby reducing the problem to that of separately diagonalizing a number of matrices of smaller dimensionality. For example, the trianion matrix breaks into pairs of blocks of dimensions 1 × 1, 4 × 4, 10 × 10, 20 × 20, 35 × 35, 53 × 53, 71 × 71, 86 × 86, and 95 × 95 corresponding to the z component of the total spin S_z' of $\pm{}^{17}/_2$, $\pm{}^{15}/_2$, $\pm{}^{13}/_2$, $\pm{}^{11}/_2$, $\pm{}^{9}/_2$, $\pm{}^{7}/_2$, $\pm{}^{5}/_2$, $\pm{}^{3}/_2$, and $\pm{}^{1}/_2$, respectively. The resulting energy levels E_n correspond to eigenfunctions of total spin $|S_n',S_{zn}'\rangle$.

With the assumption of a Boltzmann distribution for the population of the various energy levels the temperature dependence of the molar susceptibility is given by eq 3 in which

$$\chi(T) = -\frac{N}{H}\sum_n\frac{\partial E_n}{\partial H}\exp(-E_n/kT)/\sum_n\exp(-E_n/kT) \qquad (3)$$

N = Avogadro's number, H is the applied field, T is the temperature, E_n are eigenvalues, and k is Boltzmann's constant. The index n ranges over all 900 or 750 resulting energy levels for the appropriate cluster. The magnetization in Bohr magnetons is given by eq 4, where z is the direction of the applied magnetic field $\vec{H}$ and $\vec{S}_{zn}'$ is the z component of the total spin of the nth eigenstate.

$$\vec{M}(H) = \sum_n g\vec{S}_{zn}'\exp(-E_n/kT)/\sum_n\exp(-E_n/kT) \qquad (4)$$

It should be pointed out that the Hamiltonian $-2\sum J_{ij}\vec{S}_i\cdot\vec{S}_j$ is only an approximation to the interaction energy between atoms with unpaired spins. Dirac[13,14] first showed that for a system of m electrons distributed among m mutually orthogonal one-electron orbitals the spin-dependent part of the interaction energy is given as a first-order approximation by eq 5, where $\hat{s}_k$ is the spin of the kth electron. If all the orbitals on the same center are identical, the above Hamiltonian is

(13) P. A. M. Dirac, *Proc. R. Soc. London, Ser. A*, **123**, 714 (1929).
(14) P. A. M. Dirac, "The Principles of Quantum Mechanics", Oxford University Press, London, 1947, Chapter 9.

$$\mathcal{H}_{ex} = -2 \sum_{\substack{\text{electron} \\ \text{pairs } k,l}} J_{kl}\hat{s}_k \cdot \hat{s}_l \quad (5)$$

expressed by eq 6 in which $\vec{S}_i \cdot \vec{S}_j = \sum_k \hat{s}_{ik} \cdot \sum_l \hat{s}_{jl}$ and the sum-

$$\mathcal{H}_{ex} = -2 \sum_{\substack{\text{atom} \\ i,j}} J_{ij}\vec{S}_i \cdot \vec{S}_j \quad (6)$$

mation is now over pairs of centers (atoms) rather than pairs of electrons. In the case of $[Fe_4S_4(SR)_4]^{2-,3-}$ clusters the Fe(II,III) atoms are subject to local tetrahedral ligand fields causing splitting of the 3d orbitals in e and t_2 sets. Because the individual one-electron orbitals of each atom are nonidentical and the further requirement that all atoms are in orbital singlet ground states[15] is satisfied only by Fe(III), the simple isotropic exchange Hamiltonian (6) does not rigorously apply. Thus, the model should become less satisfactory as the Fe(II) character of the cluster is increased, as observed in passing from the oxidized to the reduced clusters (vide infra). With recognition of its limitations the model is applied as the simplest feasible method of analysis allowing, at the least, parameterization and qualitative comparison of the strengths of the exchange interaction in the $[Fe_4S_4(SPh)_4]^{2-,3-}$ clusters.

Analysis and Results

Descriptions of the compounds, the measurements of the magnetic susceptibility and magnetization data, and the incorporation of impurity corrections to the susceptibility data have been published elsewhere.[5]

A. $[Fe_4S_4(SPh)_4]^{2-}$. Susceptibility data for $(Et_4N)_2[Fe_4S_4(SPh)_4]$ are presented in Table I and Figure 2. Susceptibilities per tetrameric unit are given in all cases. The plotted values in Figure 2 have been corrected for the temperature-independent paramagnetism (TIP) estimated at 440 $\times 10^{-6}$ cgsu.[5] Also shown in Figure 2 are theoretical $\chi(T)$ curves generated from the spin-coupling Hamiltonian of eq 2 applied to the basis set of localized spin states $S_1 = S_2 = {}^5/_2$, $S_3 = S_4 = 2$ corresponding to the formal Fe oxidation states of the oxidized cluster. Negative J values result in a diamagnetic $S' = 0$ ground state with low-lying excited states being populated at higher temperatures. The best simulation for $[Fe_4S_4(SPh)_4]^{2-}$ with $g = 2$ as determined by visual comparison of the experimental data and the theoretical curves was obtained with the unique set of parameters $J_1 = J_{ij}(Fe^{3+} \rightleftarrows Fe^{3+}) = -275$ cm^{-1} and $J_2 = J_{ij}(Fe^{2+} \rightleftarrows Fe^{2+}) = -225$ cm^{-1}. For the minimization of the number of free parameters, cross coupling between Fe(III) and Fe(II) was given a value $J_3 = J_{ij}(Fe^{3+} \rightleftarrows Fe^{2+}) = -250$ cm^{-1}, equal to $(J_1 + J_2)/2$. Thus a fairly accurate reproduction of the experimental data is obtained with two independent parameters. For comparison the best simulation obtained with a single value of J, -232 cm^{-1}, and $g = 2$ is also shown.

B. $[Fe_4S_4(SPh)_4]^{3-}$. Susceptibility data for $(Et_4N)_3[Fe_4S_4(SPh)_4]$ are given in Table I and are plotted in Figure 3. Theoretical curves calculated by diagonalization of the energy level matrix obtained with the exchange Hamiltonian of eq 2 operating on the basis set $S_1 = {}^5/_2$, $S_2 = S_3 = S_4 = 2$ are also shown. For all J_{ij} equal, the Hamiltonian of eq 2 cannot even qualitatively reproduce the experimentally observed temperature dependence of the magnetic susceptibility for the cluster. A representative curve for a single value of the exchange integral $J = -20$ cm^{-1} with $g = 2$ is shown. It is seen that a single J value predicts a very sharp decrease of χ with increasing temperatures below $\sim$25 K and almost no variation for $T > 50$ K.

Calculations with two independent J values, $J_1 = J_{ij}(Fe^{3+} \rightleftarrows Fe^{2+})$ and $J_2 = J_{ij}(Fe^{2+} \rightleftarrows Fe^{2+})$, are in qualitative agreement with the overall behavior of the $\chi(T)$ data. The introduction of two J values in the Hamiltonian described by eq 2 results in a partial lifting of the degeneracy of the S_z' energy levels within each total spin S' manifold, thereby causing a broader distribution of states in energy space and a smoother χ vs. T variation. A systematic search in J_1, J_2 parameter space between -5 and -200 cm^{-1} was undertaken. The theoretical curve calculated with $J_1 = -60$ cm^{-1}, $J_2 = -40$ cm^{-1}, and $g = 2$ gives a reasonable simulation of the data. The sensitivity of the simulated $\chi(T)$ curve shape to changes in J_1 and J_2 is also seen in Figure 3. The inability to fit accurately the low-temperature data reflects the importance of the mixing of states with differing S_z'. This mixing results from rhombic distortions of the tetrahedral ligand fields experienced by the iron atoms and is not taken into account in eq 2. The deviation between theory and experiment is expected to be particularly noticeable at low temperature when the expectation value of the spin at each iron site differs from its full $S = {}^5/_2$ and $S = 2$ value for Fe^{3+} and Fe^{2+}, respectively. Thus the values of J_{ij} obtained must be viewed as giving the correct order of magnitude of the strength of the exchange interaction in this system, within the limitations of the theoretical assumptions.

Searches in J_1, J_2 parameter space for the best simulation of the $\chi(T)$ data revealed that reasonable simulations were obtained with nonunique J_1 and J_2 values. However, the uniquely best set can be selected by imposition of the added constraint that the values of J_1, J_2 that produce acceptable simulations of the $\chi(T)$ data (eq 3) also produce acceptable simulations of the $M(H)$ data (eq 4). Only the set $J_1 = -60$ cm^{-1} and $J_2 = -40$ cm^{-1} satisfies this criterion. The simulation of the magnetization data with these parameters is shown in Figure 4.

The resulting energy level diagram for eq 2 with these values of J_1 and J_2 is shown in Figure 5, column B, in which the low-lying states are also shown separated on the basis of total spin S'. This diagram may be contrasted with those obtained from eq 2 with single J values, $J = -40$ cm^{-1} (column A) and $J = -60$ cm^{-1} (column C). Thus comparison shows that the introduction of two inequivalent J values leads to a partial lifting of the degeneracy of the states within a total spin manifold,[17] and a consequent complexity of the low-energy excitation spectrum.

Magnetization properties of $[Fe_4S_4(SR)_4]^{3-}$ salts in the solid state are dependent upon identity of R and the quaternary ammonium countercation.[7,8] None of these compounds exhibit saturation behavior at 4.2 K and applied fields up to 50 kOe, but their saturation moments can be obtained with reasonable confidence by extrapolation. If these data are taken together with other electronic properties, clusters that approach 1 μ_B (e.g., $(Et_4N)_3[Fe_4S_4(SPh)_4]$, Figure 4) have an elongated tetragonal structure whereas those approaching 3 μ_B (e.g., $(Et_4N)_3[Fe_4S_4(SCH_2Ph)_4]$) are associated with nontetragonal structures. Detailed arguments are given elsewhere.[5,7] In this context it is interesting to observe that the exchange Hamiltonian of eq 2 yields lowest lying states having $S' = {}^1/_2$ only for negative J_1 and J_2 differing by $\lesssim 35\%$. When this difference exceeds 35%, states of an $S' = {}^3/_2$ spin manifold become the lowest lying states. As the percent difference between J_1 and J_2 is increased to much higher values, states having $S' = {}^5/_2$ eventually become the lowest lying states.

(15) A. P. Ginsberg, *Inorg. Chim. Acta, Rev.*, **5**, 45 (1971).
(16) W. E. Hatfield, in "Mixed-Valence Compounds", D. B. Brown, Ed., Reidel Publishing Co., Dordrecht, Holland, 1980, pp 191–241.
(17) Gayda et al.[18] have analyzed the temperature dependences of the EPR spectra of several reduced iron–sulfur proteins in terms of relaxations via a single excited state at energy 110 cm$^{-1} < \Delta < 300$ cm^{-1}. Using a similar procedure, we have reanalyzed our EPR data[8] for $[Fe_4S_4(SPh)_4]^{3-}$, affording $\Delta = 170$ cm^{-1}. However, the presence of many low-lying states in the calculated energy level diagram (Figure 5, column B) complicates the interpretation and probably invalidates single-parameter analyses in these systems.
(18) J. P. Gayda, P. Bertrand, C. More, J. Le Gall, and R. C. Camack, *Biochem. Biophys. Res. Commun.*, **99**, 1265 (1981).

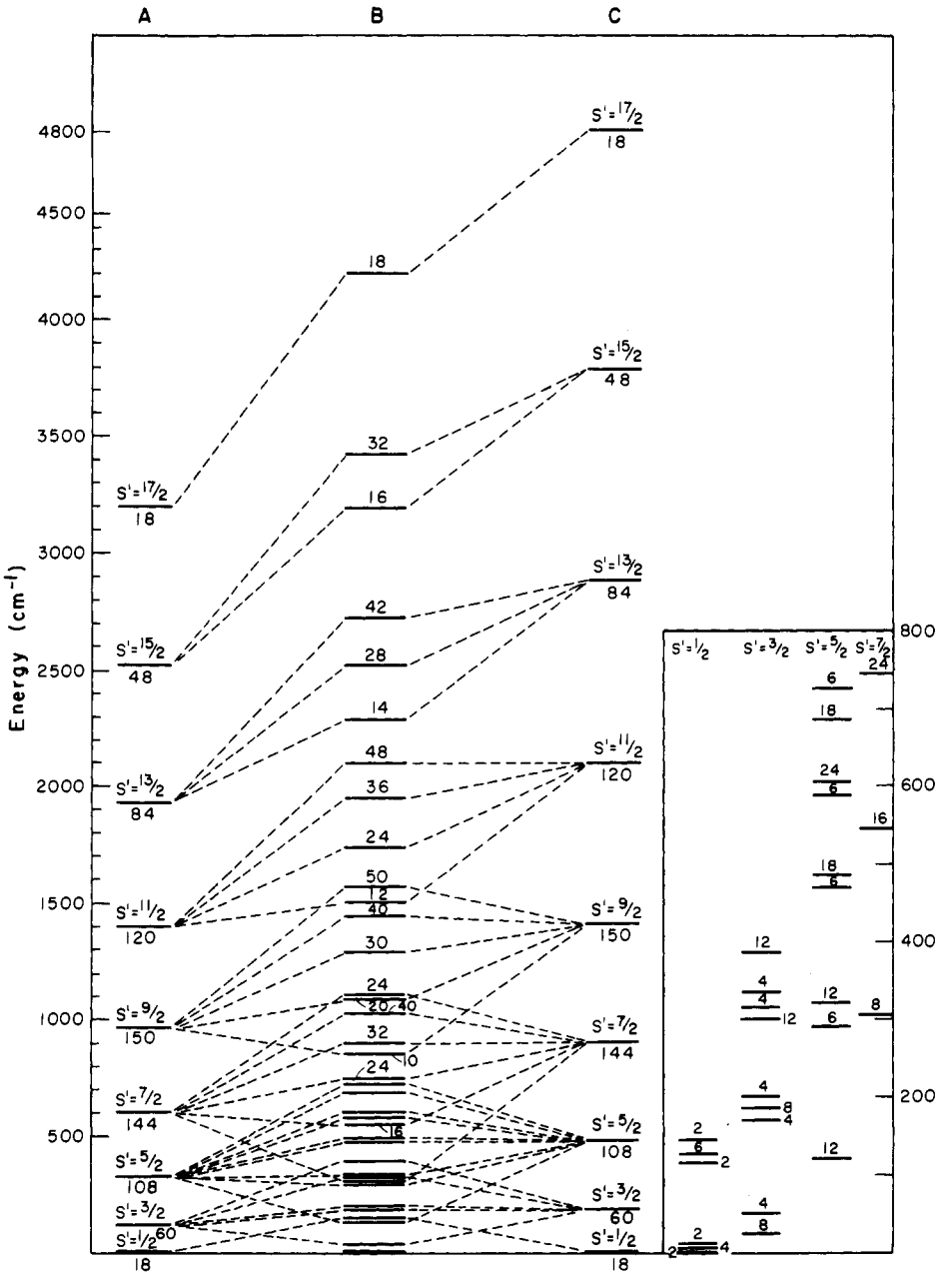

Figure 5. Energy level diagram of states resulting from the Heisenberg exchange Hamiltonian (eq 2). Column A corresponds to $J_1 = J_2 = -40$ cm^{-1}; column C corresponds to $J_1 = J_2 = -60$ cm^{-1}; column B corresponds to $J_1 = -60$ cm^{-1}, $J_2 = -40$ cm^{-1}. States below 800 cm^{-1} in column B are reproduced in the inset, separated on the basis of total spin. Integers in the diagram indicate multiplicities.

A more rigorous treatment within the spin Hamiltonian approach would require the introduction of axial and rhombic zero-field splitting terms for each iron site. This, however, introduces a computational difficulty because the resulting mixing of states of differing S_z' requires the diagonalization of a 750 × 750 matrix. Furthermore, the increase in the number of independent parameters would make conclusions drawn from such a simulation less meaningful. The present treatment, while approximate, is the most extensive analysis attempted for a tetranuclear cluster containing nonequivalent coupled spins.[19] This subject has been reviewed.[12,16]

Discussion

The observation of a reduction in the magnitude of the exchange constants as the oxidation state of the cluster is reduced is qualitatively consistent with Anderson's theory of superexchange.[20] According to this theory the metal d orbitals, in which the unpaired spins originate, overlap with filled s and p orbitals of intermediary atoms, i.e., sulfur atoms in this case. As a consequence of this overlap the orbitals containing the unpaired spins are no longer localized atomic d orbitals, but molecular orbitals that encompass both iron and sulfur atoms. The spin in two such delocalized 3d orbitals, originating from two different metal atoms, interact to couple the spins parallel or antiparallel in the low-energy state. In the case of superexchange, antiparallel coupling is most common and results from orbital overlap. The exchange integral is given by eq 7 in which b_{ij} is the transfer integral, which gives

$$J_{ij} = -b_{ij}^2/U \qquad (7)$$

a measure of the degree of orbital overlap, and U is the Coulomb repulsion of the electrons when they are all on one atom. Assuming U of a free ion and including corrections for

(19) For a treatment of spin coupling in $MoFe_3S_4$-type clusters cf. G. Christou, D. Collison, C. D. Gorner, and F. E. Mobbs, *Inorg. Nucl. Chem. Lett.*, **17**, 137 (1981).

(20) P. W. Anderson, *Phys. Rev.*, **115**, 2 (1959).

valence, nearest-neighbor, and polarization effects, Anderson[20] arrived at rough estimates of $U \approx 10$ eV for Fe^{3+} and $U \approx 5$ eV for Fe^{2+}, which interpolate to an average of ~7.5 and 6.25 eV for the dianion and trianion clusters studied in this work. Thus the fivefold difference in the strength of J_{ij} between the two oxidation states is likely due to greater transfer integrals b_{ij} for the dianion. This would imply greater electron delocalization in the dianion, a behavior not inconsistent with Mössbauer results, which indicate strict equivalence of iron sites in the oxidized, but not in the reduced, clusters.[5,7,10,11]

Quantitative calculations of exchange constants from first principles require detailed electronic structure calculations of transition-metal complexes.[21,22] The work of Ginsberg[22] on $[Mo_2Cl_9]^{3-}$ is a recent case in point. With reference to Fe–S complexes the only such calculations are for $[Fe_2S_2(SH)_4]^{2-,3-}$, simple models of the oxidized and reduced $[Fe_2S_2(Cys\text{-}S)_4]$ Fd sites, by Norman et al.[23] Xα valence bond theory predicts a reduction of J from -265 cm^{-1} in the oxidized (2 Fe(III)) to -76 cm^{-1} in the reduced (Fe(III) + Fe(II)) form if equivalent Fe centers are assumed. The calculated values are in rather good agreement with results obtained by analysis of experimental $\chi(T)$ data of one analogue[24] and several $Fd_{ox,red}$[25] proteins using a simple exchange Hamiltonian of the form $-2JS_1 \cdot S_2$: oxidized, -148 to -185 cm^{-1}; reduced, $\lesssim -100$ to -115 cm^{-1}. Yang et al.[26] have presented a preliminary electronic structure calculation of $[Fe_4S_4(SCH_3)_4]^{2-}$ by the Xα–scattered wave method. Further calculations[27] show that addition of an electron to the lowest unoccupied ($10t_2$) orbital affects states lying below it that correspond to Fe–Fe or Fe–S molecular orbitals with predominant metal 3d character. Although the exchange integrals and coupling constants were not calculated, these predicted changes in orbitals of 3d character suggest modifications in the overlap integrals upon addition of the last electron.

Finally, negative spin-exchange interactions and consequent antiferromagnetic behavior are a consistent property of $[Fe_4S_4(Cys\text{-}S)_4]$ protein sites with core oxidation levels $[4Fe\text{–}4S]^{3+,2+,1+}$. This behavior has been directly observed by magnetic susceptibility measurements (3+, 2+)[28,29] and has been deduced from temperature dependencies of EPR (3+)[30] and ^{1}H NMR (3+, 2+, 1+)[31] spectra. In addition, magnetic hyperfine interactions of opposite sign have been observed in Mössbauer spectra (3+, 1+).[32] For the reduced protein from *Chromatium* (2+) the estimate $-J \lesssim 200$ cm^{-1} has been obtained.[28] Presently available protein susceptibility data are, however, insufficiently extensive to permit meaningful application of the analysis procedure used here. Accurate $\chi(T)$ and $\vec{M}(H)$ results for proteins with the $[4Fe\text{–}4S]^+$ oxidation level would be of substantial interest as a subject for interpretation by the model developed here, because of the sensitivity of both to core structural differences in $[Fe_4S_4(SR)_4]^{3-}$ analogues. In particular, magnetization properties at cryogenic temperatures have the potential of distinguishing between tetragonal and nontetragonal core structures of 4-Fe sites in Fd_{red} proteins. On the basis of the significant work of Johnson et al.[33] magnetization information can be obtained from field and temperature dependence of protein MCD spectra. No crystallographic results are available for any reduced protein.

Acknowledgment. We are pleased to acknowledge W. O. Gillum, S. Foner, and K. H. Johnson for useful discussions. D. Sarachik advised on technical computation procedures. We thank J. P. Gayda for a communication concerning EPR results. The Francis Bitter National Magnet Laboratory is supported by the National Science Foundation. Research by E.J.L. and R.H.H. has been supported by NIH Grants GM 22352 and GM 28856.

Registry No. $[Et_4N]_2[Fe_4S_4(SPh)_4]$, 55663-41-7; $[Et_4N]_3[Fe_4S_4(SPh)_4]$, 63115-82-2.

(21) J. C. Slater, *J. Phys., Colloq. (Orsay, Fr.)*, **33**, 3 (1972).
(22) A. P. Ginsberg, *J. Am. Chem. Soc.*, **102**, 111 (1980).
(23) J. G. Norman, Jr., P. B. Ryan, and L. Noodleman, *J. Am. Chem. Soc.*, **102**, 4279 (1980).
(24) W. O. Gillum, R. B. Frankel, S. Foner, and R. H. Holm, *Inorg. Chem.*, **15**, 1095 (1976).
(25) R. E. Anderson, W. R. Dunham, R. H. Sands, A. J. Bearden, and H. L. Crespi, *Biochim. Biophys. Acta*, **408**, 306 (1975); G. Palmer, W. R. Dunham, J. A. Fee, R. H. Sands, T. Lizuka, and T. Yonetani, *ibid.*, **245**, 201 (1971); L. Petersson, R. Cammack, and K. K. Rao, *ibid.*, **622**, 18 (1980).
(26) C. Y. Yang, K. H. Johnson, R. H. Holm, and J. G. Norman, Jr., *J. Am. Chem. Soc.*, **97**, 6596 (1975).
(27) K. W. Johnson, private communication (unpublished results).
(28) B. C. Antanaitis and T. H. Moss, *Biochim. Biophys. Acta*, **405**, 262 (1975).
(29) M. Cerdonio, R.-H. Wang, J. Rawlings, and H. B. Gray, *J. Am. Chem. Soc.*, **96**, 6534 (1974).
(30) H. Blum, J. C. Salerno, R. C. Prince, J. S. Leigh, Jr., and T. Ohnishi, *Biophys. J.*, **20**, 23 (1977).
(31) W. D. Phillips, M. Poe, C. C. McDonald, and R. G. Bartsch, *Proc. Natl. Acad. Sci. U.S.A.*, **67**, 682 (1970); M. Poe, W. D. Phillips, C. C. McDonald, and W. Lovenberg, *ibid.*, **65**, 797 (1970); W. D. Phillips, C. C. McDonald, N. A. Stombaugh, and W. H. Orme-Johnson, *ibid.*, **71**, 140 (1974); M. Poe, W. D. Phillips, C. C. McDonald, and W. H. Orme-Johnson, *Biochem. Biophys. Res. Commun.*, **42**, 705 (1971); C. C. McDonald, W. D. Phillips, W. Lovenberg, and R. H. Holm, *Ann. N.Y. Acad. Sci.*, **222**, 789 (1973).
(32) P. Middleton, D. P. E. Dickson, C. E. Johnson, and J. D. Rush, *Eur. J. Biochem.*, **88**, 135 (1978); **104**, 289 (1980).
(33) M. K. Johnson, A. J. Thomson, A. E. Robinson, K. K. Rao, and D. O. Hall, *Biochim. Biophys. Acta*, **667**, 443 (1981).